

# Radicals Formed in *N*-Acetylproline by Electron Attachment: Electron Spin Resonance Spectroscopy and Computational Studies

Jeanette F. Kheir,<sup>†</sup> Lidia Chomicz,<sup>‡</sup> Janusz Rak,<sup>‡</sup> Kit H. Bowen,<sup>§</sup> and Michael D. Sevilla<sup>†,\*</sup>

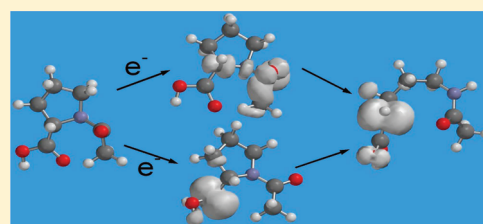
<sup>†</sup>Department of Chemistry, Oakland University, Rochester, Michigan 48309, United States

<sup>‡</sup>Department of Chemistry, University of Gdańsk, 80-952 Gdańsk, Poland

<sup>§</sup>Department of Chemistry, Johns Hopkins University, Baltimore, Maryland 21218, United States

 Supporting Information

**ABSTRACT:** In this study, the reactions of electrons with *N*-acetylproline are investigated by electron spin resonance (ESR) spectroscopy and density functional theory. Electrons are produced by  $\gamma$  irradiation or by photoionization of  $K_4Fe(CN)_6$  in neutral 7.5 M LiCl–D<sub>2</sub>O aqueous glasses at low temperatures with identical results. Electrons are found to add to both the peptide bond and the carboxyl group of the acetyl-proline moiety at 77 K. On annealing, both the electron adducts undergo fragmentation of the peptide bond between the nitrogen and the  $\alpha$  carbon of the peptide structure. However, the peptide bond electron adduct radical reacts much more rapidly than the carboxyl group electron adduct radical. The DFT calculations predict that the carboxyl adduct is substantially more stable than the peptide bond adduct, with the activation barrier to N–C $\alpha$  cleavage 3.7 kcal/mol for the amide electron adducts and 23 kcal/mol for the carboxyl electron adducts in agreement with the relative reactivity found by experiment.



## 1. INTRODUCTION

Low energy and solvated electrons are a principle product of water radiolysis induced by high energy radiation ( $X$  or  $\gamma$ ).<sup>1</sup> On addition to DNA and protein structures such electrons cause damage chiefly by bond cleavage reactions.<sup>2–4</sup> For example, in peptides electron attachment usually causes fragmentation of the N-terminal amine group or the peptide bond. However, proline, which has a cyclic structure, is unusual in its behavior: in mass spectrometry experiments carried out for two dipeptides, Gly-Pro and Pro-Gly, no fragmentation was observed for the first case, whereas the characteristic dissociation products of the N–C $\alpha$  bond were observed for the latter one. This “proline effect” was ascribed to proline ring-opening on N–C $\alpha$  cleavage which still leaves the peptide connected in Gly-Pro but not in Pro-Gly.<sup>5</sup>

A number of previous studies has investigated radicals formed by the reaction of electrons with amino acids, *N*-acetyl amino acids and peptides or model systems in a neutral aqueous glasses<sup>6–8</sup> and alkaline glasses<sup>9–11</sup> and showed that on attachment electrons induce a number of fragmentation reactions in these aqueous systems. Studies of direct  $\gamma$  irradiation of *N*-acetyl amino acids in frozen aqueous solutions<sup>12</sup> resulted in radicals from both electron and holes in the structure. The electron induced reactions in the frozen ices followed the chemistry similar to those in aqueous glasses.

In current studies we investigate the reactions of electrons with *N*-acetylproline (*N*-AcPro) as it is the smallest proline-like structure containing a peptide bond and acts as the simplest model for the proline in a protein backbone (Scheme 1). In an allied work, electron attachment to *N*-AcPro in the gas phase was

investigated by photoelectron spectroscopy and, although the valence anion and its valence electron affinity were found, no evidence for cleavage was observed.<sup>13</sup> In this work electron reactions are investigated in aqueous glasses at low temperatures and theoretical DFT calculations of the electron adducts and reaction products were performed for comparison to experiment. Results clearly show that cleavage of the N–C $\alpha$  bond is the dominant pathway in aqueous media. However, proline’s cyclic nature prevents full cleavage of the protein chain which is an important characteristic. Because proline is an important amino acid in structural components such as cartilage this characteristic of requiring two cleavages to break a protein chain is likely instrumental in maintaining the integrity of these biological structures.

## 2. MATERIALS AND METHODS

**Experiment.** *N*-AcPro used in these experiments was purchased from Sigma-Aldrich as were the lithium chloride,  $\geq 99\%$  (LiCl) and deuterium oxide, 99.9% (D<sub>2</sub>O), used to prepare 7.5 M LiCl/D<sub>2</sub>O. The employed  $\gamma$  (Co-60) irradiator was GR-9, producing 1.0 kGy/h. The UV source was a low pressure Xe–Hg lamp producing most of its intensity in the 254 nm range. All samples were irradiated at 77 K. The ESR (electron spin resonance) spectrometer was E-9 Century Series with dual cavities. Suprasil quartz tubes (4 mm in diameter) were used to place the samples in and were purchased from Wilmad Labglass.

**Received:** August 15, 2011

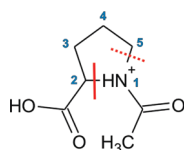
**Revised:** October 6, 2011

**Published:** November 01, 2011

Potassium ferrocyanide ( $K_4Fe(CN)_6 \cdot 3H_2O$ ) was purchased from Mallinckrodt.

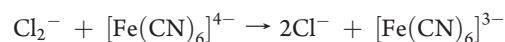
**Sample Preparation.** Approximately 5 mg (50 mM) of the *N*-acetylproline  $\cdot HCl$  was dissolved in 0.5 mL of 7.5 M  $LiCl/D_2O$ . The sample pH was near 2; however, on adjusting to pH 7 and 9 similar results were found. Approximately 2 mg (10 mM) of potassium ferrocyanide ( $K_4Fe(CN)_6$ ) was added for samples intended to be UV radiated.<sup>9</sup> After the solution was fully dissolved, it was bubbled with nitrogen gas to remove oxygen from the sample. The sample was then drawn into a 4 mm quartz

**Scheme 1. Structure of *N*-Acetylproline (*N*-AcPro) Showing the Preferred Cleavage Site at  $N-C_\alpha$  (N1–C2) after Electron Addition Which Occurs at Both the Carboxyl and Acetyl Groups<sup>a</sup>**



<sup>a</sup> The second dashed line shows an alternative cleavage site not found in this work.

tube and cooled to 77 K in liquid nitrogen to form a clear glass. To eliminate the possibility that the  $Cl_2^-$  formed on  $\gamma$  irradiation of the aqueous glass was contributing to radical formation in *N*-AcPro on annealing, in several samples  $K_4Fe(CN)_6$  was added to the 7 M  $LiCl$  solution before irradiation. In these samples  $Cl_2^-$  is scavenged on annealing of samples to 150 K by one electron oxidation of  $[Fe(CN)_6]^{4-}$  as shown below.



We found the same results with and without added ferrocyanide, which suggests attack by  $Cl_2^-$  did not contribute to the radical production on annealing.

**Radical Formation.** The samples were  $\gamma$  irradiated with Co-60 source for ca. 60 krad or UV irradiated with 254 nm light from a low pressure helical mercury vapor lamp for 1–2 min. After irradiation, an ESR spectrum was taken to view radicals produced from  $\gamma$  irradiation or UV radiation. Annealing of the sample at temperatures of 152–170 K was performed to view thermally induced radical reactions. Continued UV irradiation for long exposure times results in photolysis of the radicals and therefore photolysis times were restricted to 2 min.

**Computations.** The names of *N*-AcPro cations are preceded with a prefix “cat”. Because *N*-AcPro may exist in several

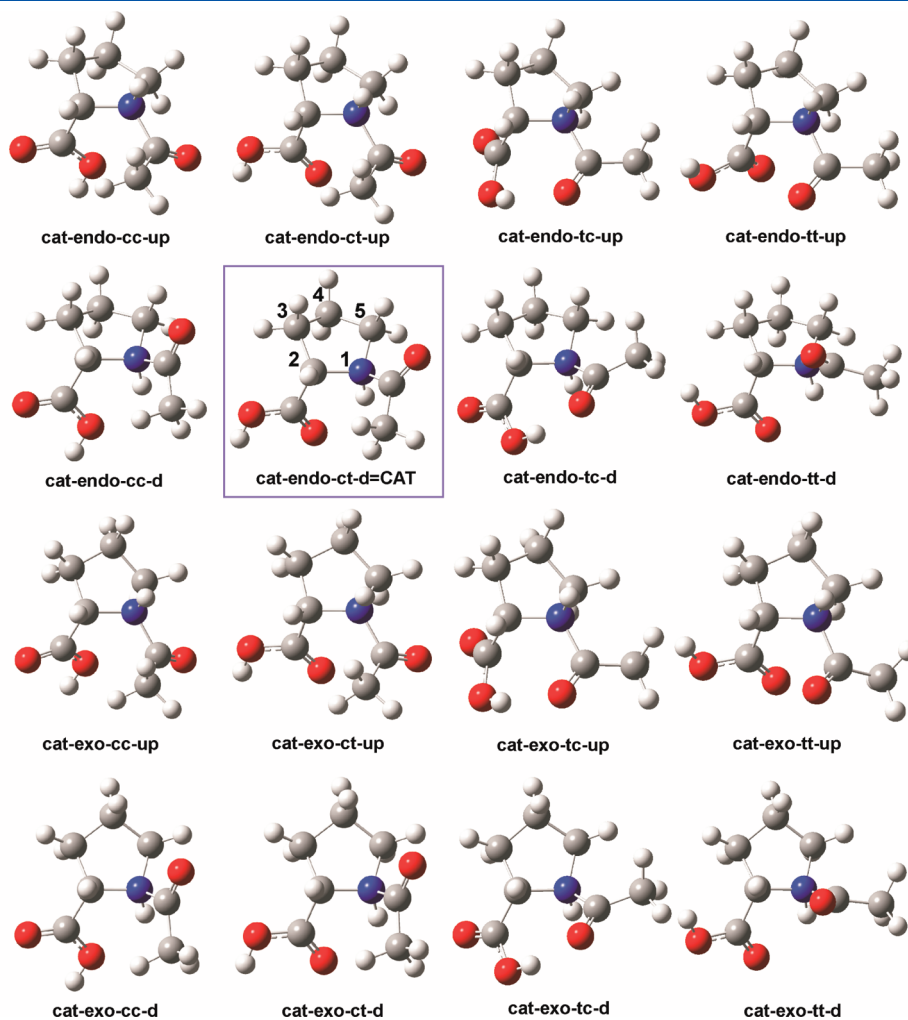


**Figure 1.** Geometries of the *N*-AcPro (*N*-acetylproline) cationic conformers. The most thermodynamically stable one is framed and has the pyrrolidine ring numbering scheme.

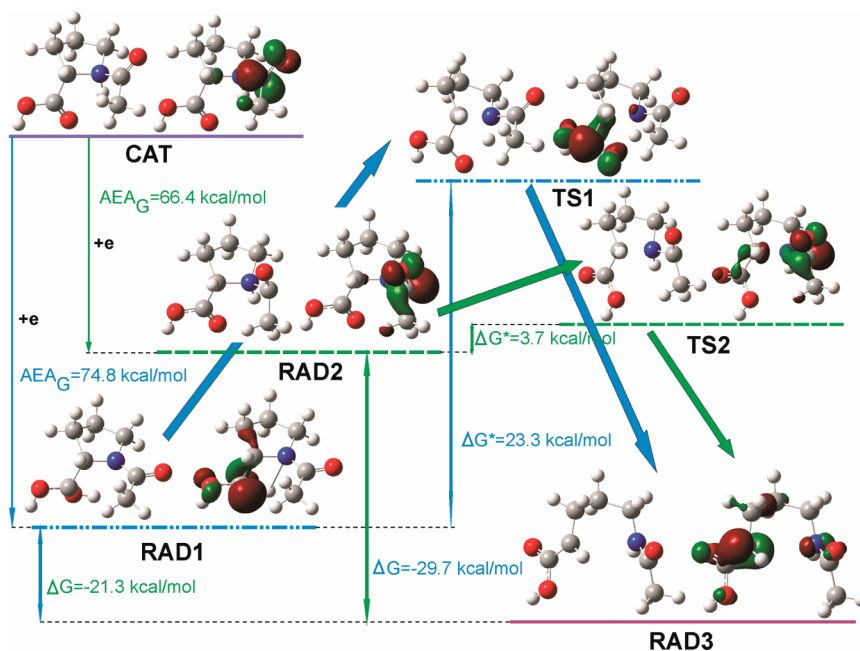


**Figure 2.** Geometries and singly occupied molecular orbitals (SOMO) distribution in stationary points (radical substratum, RAD1 and RAD2; transition states, TS1 and TS2; product, RAD3) on the reaction paths, concerning the N1–C2 bond splitting in the cationic *N*-AcPro, after electron attachment to cationic *N*-AcPro (CAT).  $\Delta G$ ,  $\Delta G^*$ , and  $AEAG$  denote the free energy of reaction, the activation free energy, and adiabatic electron affinity in free energy scale, respectively. SOMO orbitals plotted with a contour value of  $0.06 \text{ bohr}^{-3/2}$ .

conformations, as demonstrated by Aliev et al. in their conformational NMR studies,<sup>14,15</sup> “-endo-“ and “-exo-“ are used to differentiate between the  $C^{\gamma}$ -endo and  $C^{\gamma}$ -exo ring conformers, respectively (Figure 1). Furthermore, the cis and trans rotamers of *N*-AcPro (related to the acetyl group rotation with respect to the *N*-AcPro ring) are indicated by a suffix “-c-“ and “-t-“, respectively. The cis and trans position of the carboxyl group is indicated by a suffix “-c-“ or “-t-“, respectively (Figure 1). Finally, a suffix at the end of the name is related to proton attached in acid conditions, directed upward (“-up”) or downward (“-d”) with respect to pyrrolidine’s ring. For instance, “cat-endo-ct-up” stands for a cation conformer in which the pyrrolidine ring, the acetyl, the carboxyl group, and the acid proton assume  $C^{\gamma}$ -endo, cis, trans, and upward conformations, respectively.

There are two possible radicals, created by electron attachment to the cation: carboxyl type radical, named “RAD1” and acetyl type radical, named “RAD2”. Transition states, leading from these radicals to the broken ring products (“RAD3”), are marked with “TS1” and “TS2”, respectively (Figure 2).

We have applied the density functional theory method with the Becke’s three-parameter hybrid functional (B3LYP)<sup>16–18</sup> and the 6-31++G(d,p) basis set.<sup>19,20</sup> Additionally, to simulate an aqueous environment, the polarized continuum model (PCM)<sup>21</sup> with the UAHF solvation radii<sup>22</sup> was employed.

All geometries presented here were fully optimized without any geometrical constraints, and the analysis of harmonic frequencies proved that all of them are either structures at energetic minima (all force constants positive) or first-order saddle points (all but one force constants positive). The relative energies ( $\Delta E$ ) and free energies ( $\Delta G$ ) of cations were defined with respect to the most stable one (cat-endo-ct-d = CAT). Moreover, the difference in Gibbs free energy between the most stable cation entity and its radicals both in their correspondingly fully relaxed structures is denoted by  $AEAG$ . The relative energies

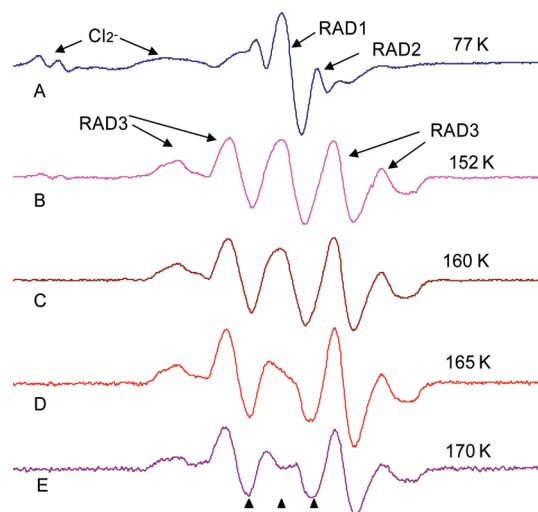


**Figure 3.** ESR spectra of *N*-AcPro in 7.5 M LiCl after 45 min of  $\gamma$  irradiation at 77 K. (A) Sample at 77 K showing electron adducts RAD1 and RAD2. (B) Sample after annealing to 152 K for 15 min which converts RAD1 and RAD2 to RAD3. Gradual annealing from 152 K (B) to 170 K (E) results in further loss of RAD1 and formation of RAD3. After annealing to 170 K for 10 min, the spectrum is entirely due to RAD3. The three markers are separated by 13.09 G each. The middle marker is at  $g = 2.0056$ . All spectra were recorded at 77 K after annealing to temperatures shown in the figure.

( $\Delta E$ ) and free energies ( $\Delta G$ ) as well as activation energies ( $\Delta E^*$ ) and free energies ( $\Delta G^*$ ) are calculated with respect to RAD1 and RAD2.

All quantum chemical calculations were carried out with the GAUSSIAN03<sup>23</sup> code on dual Intel Itanium 2 nodes at the Academic Computer Center in Gdańsk (TASK) and the pictures

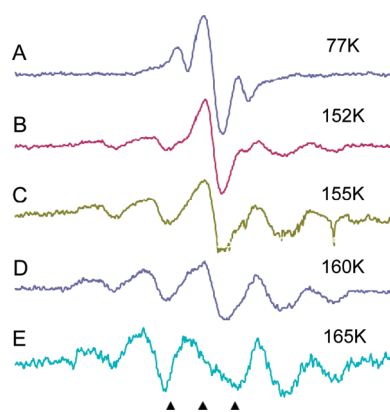


**Figure 4.** ESR spectra of *N*-AcPro in 7.5 M LiCl with  $K_4Fe(CN)_6$  after 1 min of 254 nm UV photoionization of  $K_4Fe(CN)_6$  at 77 K to produce electrons. (A) Sample immediately after UV radiation at 77 K; the photoejected electrons added to *N*-AcPro to form the electron adducts, RAD1 (the singlet in the center) and RAD2 (the doublet). (B) Sample annealed to 152 K resulting in loss of RAD2 and formation of RAD3. (C) Sample annealed to 155 K which results in the loss of RAD1 and increased formation of RAD3. (D) Sample after annealing to 160 K. (E) Sample after annealing to 165 K at which point all RAD1 has reacted. Some loss of intensity occurs due to radical–radical recombination. All spectra were recorded at 77 K after annealing to temperatures shown in the figure.

of molecules and orbitals were plotted with the GaussView 5 package.<sup>24</sup>

### 3. RESULTS AND DISCUSSION

**Experiment.** *Acetyl-DL-Proline under  $\gamma$  Irradiation.* Results of  $\gamma$  irradiation of *N*-acetylproline  $\cdot$  HCl in 7.5 M LiCl ( $D_2O$ ) at pH 2 is shown in Figure 3. The large central peak is assigned to the carboxyl electron adduct radical (RAD1) and the 24 G doublet is assigned to the peptide bond electron adduct radical (RAD2). In addition we see some initial reaction of the electron adducts to form cleavage product (RAD3, peaks in wings). The low field lines are from  $Cl_2^-$ , which do not affect the  $g = 2$  region significantly. RAD1 has a  $\beta$  proton but does not show a significant coupling because the geometry places it in the nodal plane of the carboxyl carbon p-orbital which is the dominant site of the unpaired spin (Figure 2). RAD2 shows only one coupling from the methyl group because it is in a locked configuration at 77 K (Figure 2 and vide infra). We note that the electron adducts of the peptide bond ( $pK_a = ca. 13$ )<sup>25</sup> and the carboxyl group ( $pK_a = 9.5$ )<sup>25</sup> will protonate to form neutral radicals even in neutral solutions. Experiments at pH 7 and 9 gave similar results but increased the formation of RAD2 over RAD1. Annealing of the sample to 152 K for 15 min increases the amount of RAD3 with the complete loss of RAD2 and partial loss of RAD1. Subsequent gradual annealing results in the continued loss of RAD1 until at 170 K only RAD3 is found (Figure 3E). The last spectrum shows a five-line pattern (large 44 G doublet split by a triplet of 20 G separation) resulting from one  $\beta$  proton with 44 G coupling and two protons with 20 G coupling, one of which is assigned to the  $\alpha$  proton at the radical site and the second to the  $\beta$  proton coupling on the side chain. In Figure 3E a small sharp peak between the second and third markers at  $g = 2.000$  is from a quartz background signal from  $\gamma$  irradiation of the quartz tube and not a part of the *N*-AcPro spectrum (Figure 4E in which UV light was employed does

**Table 1.** Energetic Characteristics of the Cation Conformers of *N*-AcPro Calculated at the B3LYP/6-31++G\*\* Level<sup>a</sup>

acetyl and carboxyl groups conformations	ring conformation			
	endo		exo	
	$\Delta E$	$\Delta G$	$\Delta E$	$\Delta G$
cc-up	5.36	5.45	5.50	5.75
cc-d	2.22	2.80	1.94	2.34
ct-up	3.62	3.56	3.71	3.73
ct-d	0.00	0.00	-0.13	0.15
tc-up	10.63	10.00	11.26	10.66
tc-d	7.42	6.68	7.87	7.29
tt-up	7.54	7.63	6.86	6.65
tt-d	2.33	2.61	3.16	3.49

<sup>a</sup>  $\Delta E$  and  $\Delta G$  stand for the relative electronic energy and free energy, respectively, calculated with respect to the cat-endo-ct-d structure (the lowest energy conformer); all values given in kcal/mol.

not show this peak). The overall fragmentation of the electron adduct is shown in Figure 2. The possible cleavage of the N1–C5(side chain) (for atom numbering see Figure 1) bond to form the  $\cdot CH_2CH_2CH_2-$  radical was considered, but no evidence for this species was found.

*UV Irradiation of N-Acetylproline.* The comparison of UV radiation and  $\gamma$  radiation was of interest to eliminate the possible role of  $Cl_2^-$  in radical production. Figure 4 shows spectra of radicals produced by 1 min of 254 nm UV photolysis of a sample of *N*-AcPro in 7.5 M LiCl with  $K_4Fe(CN)_6$ . The electrons photoejected from  $K_4Fe(CN)_6$  add to *N*-AcPro to form the electron adducts. The radicals produced this way were identical to those induced by  $\gamma$  radiation. The initial radicals (at 77 K) were again the carboxyl radical (RAD1) and the peptide radical (RAD2) but little cleavage reaction was found at 77 K. As found for  $\gamma$  irradiation, on progressive annealing both RAD1 (by 152 K) and RAD2 (by 165 K) are lost with the corresponding appearance of RAD3. The UV irradiated sample contains no  $Cl_2^-$  as it is formed only in  $\gamma$  irradiated samples.

**Molecular Mechanism of *N*-AcPro degradation.** *Cations.* Neutral forms of *N*-acetylproline (*N*-AcPro) are easily protonated in acidic conditions, giving the respective cations. These cations can exist in various conformer forms, differing in pyrrolidine ring shape as well as in acetyl and carboxyl groups and proton orientations (Figure 1). Among the various conformers, the most stable in terms of free energy,  $\Delta G$ , is one of the endotype, i.e., cat-endo-ct-d = CAT (Table 1 and Figure 1). This conformer was, therefore, taken under consideration in the detailed investigations.

*Reaction path.* Two types of radicals (carboxyl, RAD1; acetyl, RAD2; Figure 2) can be created due to electron attachment to the cationic *N*-AcPro. The cationic *N*-AcPro is a strong electron acceptor: for both the above-mentioned radicals adiabatic electron affinity ( $AEA_G$ ) is extremely high (ca. 70 kcal/mol; Figure 2). When the electron attaches to the carboxyl group, it loses its planarity. Moreover, a barrier-free intramolecular proton transfer (BFIPT) between the protonated pyrrolidine nitrogen and carbonyl oxygen of the carboxyl group takes place. Such BFIPT process is not possible for the radical formed due to electron attachment to the acetyl group. Thus, BFIPT accounts for

**Table 2. Theoretical and Experimental Proton Hyperfine Couplings (G) for Proline Radicals<sup>a</sup>**

radicals	DFT calculated/experimental proton couplings			
	C2–H	C3–H1	C3–H2	acetyl–CH <sub>3</sub>
RAD1	3.4/<5			
RAD2	26.1/24 <sup>b</sup> (1H)			
RAD3	–19.6/20	16.7/44	6.6/20 <sup>c</sup>	
	–19.6/20	47.4/44	20.5/20 <sup>d</sup>	

<sup>a</sup>Theoretical/experimental values. <sup>b</sup>Only one coupling from the methyl group is experimentally observed. At 77 K the methyl group is locked so to produce one large and two small experimentally not observed couplings. <sup>c</sup>Equilibrium conformation. <sup>d</sup>Couplings for a nonequilibrium conformation with dihedral C<sub>carboxyl</sub>–C2–C3–C4 = 23° that gives experimental values.

significantly larger AEA<sub>G</sub> observed for RAD1 (74.7 (RAD1) vs 66.4 (RAD2) kcal/mol; Figure 2).

Both radicals are thermodynamically stable; however, they can undergo further stabilization related to the dissociation of the ring C2–N1 bond. These reactions are exergonic for both with  $\Delta G = -21.3$  kcal/mol for RAD1 and  $\Delta G = -29.7$  kcal/mol for RAD2. Both ring-opening reactions are thermally activated, and the calculated activation barriers found are 23 kcal/mol for RAD1 and only 4 kcal/mol for RAD2 (Figure 2). The heights of these barriers are quite different because already small C2–N1 bond stretching leads to the transition state configuration for RAD2 whereas for RAD1 the C2–N1 bond stretching, proton retransferring, and the carboxyl group flattening are involved in the reaction coordinate.

**ESR Assignments.** The suggested mechanism of electron induced *N*-AcPro degradation is in good agreement with the results of the ESR experiments described previously (Figures 3 and 4). As mentioned, the singlet results from the carboxyl radical (RAD1). The electron is localized on the deformed carboxyl group (Figure 2) and does not couple with any proton magnetic moments because of the molecular geometry.

In the initial doublet from acetyl peptide radical (RAD2) the electron is localized on peptide bond (Figure 2). One would expect coupling of the unpaired electron to three protons from the methyl group as well as other couplings from nitrogen and the proton at the nitrogen. However, only one large coupling from one proton from the methyl group is found, because at low temperature, rotation of the methyl group is hindered and a single orientation is produced.<sup>11,26,27</sup> Moreover, when it comes to proton bonded with a N atom, it should be remembered that D<sub>2</sub>O was used in experiment and deuterium couplings would be too small to be observed. The doublet from RAD2 has been found previously in experiments with electron adducts of acetyl peptides, acetamide, and even acetate at 77 K. All three methyl couplings are found in acetamide and acetate only on warming to 180 K where the methyl group rotates.<sup>11,26,27</sup> No such warming cycle is possible for *N*-AcPro as RAD2 is unstable to temperature increase. We find the electron adduct to the peptide group of *N*-AcPro (RAD2) is formed in lower amounts than the RAD1 carboxyl adduct, likely because RAD1 is significantly more thermodynamically stable than RAD2. Theory shows that RAD2 disappears earlier than

RAD1 singlet because its lower thermodynamic stability as well as a significantly lower kinetic barrier to formation of RAD3.

The open-ring product RAD3 shows couplings to one  $\alpha$  proton (ca. 20 G) at C2 and two  $\beta$  protons (44 and 20 G) at C3 with different orientations to the radical site. These couplings compare well to previous results with similar molecular structures,<sup>8</sup> but not for the optimized DFT calculated hyperfine couplings shown in Table 2. Only a change in dihedral angle,  $\theta = \text{C}_{\text{carboxyl}}-\text{C2}-\text{C3}-\text{C4}$  (Scheme 1) places the two  $\beta$  protons so that the couplings agree (Table 2). The energy required for this change is small (ca. 1.9 kcal/mol) and is likely a matrix induced minimum structure.

## 4. SUMMARY

We find both the carboxyl and peptide electron adduct radicals are formed with the carboxyl adduct favored. Annealing to higher temperatures both the carboxyl and peptide electron adducts react to cleave the peptide link at the N1–C2 bond. However, the N1–C5 bond to the side chain link remains intact. The peptide electron adduct reacts far more quickly than the carboxyl adduct, and this is supported by theory that shows the carboxyl adduct to be the most stable. The method used to produce electrons was also studied, and the radicals produced with both  $\gamma$  irradiation and UV photoionization of K<sub>4</sub>Fe(CN)<sub>6</sub>, were identical. DFT calculations predict the initial radical identities, their stability, reactivity and coupling constants in good accord with experiment.

## ■ ASSOCIATED CONTENT

**S Supporting Information.** Cartesian coordinates for the constrained RAD3 geometry. This material is available free of charge via the Internet at <http://pubs.acs.org>.

## ■ AUTHOR INFORMATION

### Corresponding Author

\*E-mail: [sevilla@oakland.edu](mailto:sevilla@oakland.edu).

## ■ ACKNOWLEDGMENT

We greatly appreciate the aid of the Department of Chemistry for granting the Thompson Undergraduate Research Award (J.F.K.) and the NIH (RO1 CA 045424) for partial support of this research. This work was also supported by the Polish Ministry of Science and Higher Education (MNiSW) Grant No.: DS/8221-4-0140-1 (J.R.). The calculations were performed at the Academic Computer Center in Gdańsk (TASK). Support from the NSF under grant number is CHE-1111693 is also acknowledged (K.H.B.). Professors Amitava Adhikary, Alyson Engle, and Deepti Khanduri are acknowledged for their generous aid and helpful discussions.

## ■ REFERENCES

- (1) Ershov, B. G.; Gordeev, A. V. *Radiat. Phys. Chem.* **2008**, *77*, 928–935.
- (2) Boudaiffa, B.; Cloutier, P.; Hunting, D.; Huels, M. A.; Sanche, L. *Science* **2000**, *287*, 1658–1660.
- (3) Sanche, L. *Eur. Phys. J. D* **2005**, *35*, 367–390.
- (4) Syrstad, E. A.; Tureček, F. *J. Am. Soc. Mass Spectrom.* **2005**, *16*, 208–224.

- (5) Hayakawa, S.; Hashimoto, M.; Matsubara, H.; Tureček, F. *J. Am. Chem. Soc.* **2007**, *129*, 7936–7949.
- (6) Sevilla, M. D.; Brooks, V. L. *J. Phys. Chem.* **1973**, *77*, 2954–2959.
- (7) Sevilla, M. D.; Failor-Koszykowski, R. *J. Phys. Chem.* **1977**, *81*, 1198–1200.
- (8) Sevilla, M. D.; D'Arcy, J. B.; Suryanarayana, D. *J. Phys. Chem.* **1978**, *82*, 2589–2594.
- (9) Sevilla, M. D. *J. Phys. Chem.* **1970**, *74*, 2096–2102.
- (10) Sevilla, M. D. *J. Phys. Chem.* **1970**, *74*, 3366–3372.
- (11) Sevilla, M. D. *J. Phys. Chem.* **1970**, *74*, 669–672.
- (12) (a) Sevilla, M. D.; D'Arcy, J. B.; Morehouse, K. M. *J. Phys. Chem.* **1979**, *83*, 2893–2897. (b) Sevilla, M. D.; D'Arcy, J. B.; Morehouse, K. M. *J. Phys. Chem.* **1979**, *83* (22), 2887–2892.
- (13) Chomicz, L.; Rak, J.; Paneth, P.; Sevilla, M. D.; Ko, Y. J.; Wang, H.; Bowen, K. H. *J. Chem. Phys.* **2011**, *135*, 114301–114307.
- (14) Aliev, A. E.; Courtier-Murias, D. *J. Phys. Chem. B* **2007**, *111*, 14034–14042.
- (15) Aliev, A. E.; Bhandal, S.; Courtier-Murias, D. *J. Phys. Chem. A* **2009**, *113*, 10858–10865.
- (16) Becke, A. D. *Phys. Rev. A* **1988**, *38*, 3098–3100.
- (17) Becke, A. D. *J. Chem. Phys.* **1993**, *98*, 5648–5652.
- (18) Lee, C.; Yang, W.; Parr, R. G. *Phys. Rev. B* **1988**, *37*, 785–789.
- (19) Ditchfield, R.; Hehre, W. J.; Pople, J. A. *J. Chem. Phys.* **1971**, *54*, 724–728.
- (20) Hehre, W. J.; Ditchfield, R.; Pople, J. A. *J. Chem. Phys.* **1972**, *56*, 2257–2261.
- (21) Tomasi, J.; Mennucci, B.; Cammi, R. *Chem. Rev.* **2005**, *105*, 2999–3093.
- (22) Barone, V.; Cossi, M.; Tomasi, J. *J. Chem. Phys.* **1997**, *107*, 3210–3221.
- (23) Frisch, M. J.; et al. *Gaussian 03*, revision B.05; Gaussian Inc.: Pittsburgh, PA, 2003.
- (24) Frisch, M. J.; Hratchian, H. P.; Dennington, R. D., II; Keith, T. A.; Millam, J. *GaussView 5*; Gaussian Inc.: Wallingford, CT, 2009.
- (25) von Sonntag, C. *Free-radical-induced DNA Damage and Its Repair (A Chemical Perspective)*; Springer-Verlag: Berlin, Heidelberg, 2006.
- (26) Suryanarayana, D.; Sevilla, M. D. *J. Phys. Chem.* **1979**, *83*, 1323–1327.
- (27) Suryanarayana, D.; Sevilla, M. D. *J. Phys. Chem.* **1980**, *84*, 3045–3049.